Half-Sandwich Complexes of an Extremely Electron-Donating, Redox-Active η⁶-Diborabenzene Ligand

Julian Böhnke,[†,‡] Holger Braunschweig,*[,†,‡] J. Oscar C. Jiménez-Halla,[§] Ivo Krummenacher[†,‡] and Tom E. Stennett[†,‡]

[†]Institute for Inorganic Chemistry, Julius-Maximilians-Universität Würzburg, Am Hubland, 97074 Würzburg, Germany

[‡]Institute for Sustainable Chemistry & Catalysis with Boron, Am Hubland, 97074 Würzburg, Germany

[§]Departamento de Química, División de Ciencias Naturales y Exactas, Universidad de Guanajuato, Noria Alta S/N, Col. Noria Alta, Guanajuato, C.P. 36050, Gto., Mexico

ABSTRACT: The heteroarene 1,4-bis(CAAC)-1,4-diborabenzene (**1**; CAAC = cyclic (alkyl)(amino)carbene) reacts with $[(MeCN)_3M(CO)_3]$ (M = Cr, Mo, W) to yield half-sandwich complexes of the form $[(\eta^6\text{-diborabenzene})M(CO)_3]$ (M = Cr (**2**), Mo (**3**), W (**4**)). Investigation of the new complexes with a combination of X-ray diffraction, spectroscopic methods and DFT calculations shows that ligand **1** is a remarkably strong electron donor. In particular, $[(\eta^6\text{-arene})M(CO)_3]$ complexes of this ligand display the lowest CO stretching frequencies yet observed for this class of complex. Cyclic voltammetry on complexes **2**-**4** revealed one reversible oxidation and two reversible reduction events in each case, with no evidence of ring-slippage of the arene to the η^4 binding mode. Treatment of **4** with lithium metal in THF led to identification of the paramagnetic complex [(**1**)W(CO)$_3$]Li·2THF (**5**). Compound **1** can also be reduced in the absence of a transition metal to its dianion $\mathbf{1}^{2-}$, which possesses a quinoid-type structure.

Half-sandwich complexes of arenes are among the most well-known of all organometallic compounds. Since the isolation of $[(\eta^6\text{-}C_6H_6)Cr(CO)_3]$ by Fischer and Öfele in 1957 (Figure 1), the discovery that coordination to the $Cr(CO)_3$ fragment makes arenes susceptible to nucleophilic substitution has been instrumental in organic synthesis.[1-2] Although less well studied than their all-carbon analogues, a variety of heteroarene complexes of the Group 6 $M(CO)_3$ series are also known. Pyridines, typically η^1 donor ligands, can be coerced into η^6 coordination by use of bulky substituents in the 2 and 6 positions,[3-4] while half-sandwich complexes of η^6 phosphabenzene,[5-7] arsabenzene,[8-9] and stibabenzene[9] ligands have also been reported. Silabenzenes[10] and germabenzenes,[11] kinetically stabilised by large substituents, have also been coordinated to group 6 tricarbonyl fragments.

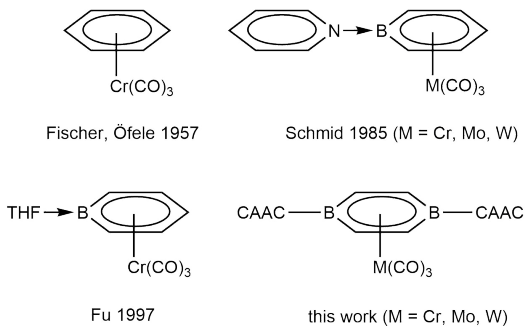

Figure 1. Selected Group 6 arene and heteroarene tricarbonyl complexes.

Of the boron derivatives,[12] neutral borabenzenes,[13-14] in which a CH fragment of benzene is replaced by B, require stabilisation from a Lewis base for their isolation. These are distinguished from boratabenzenes, which contain an exocyclic, covalently bonded substituent at boron and possess an overall negative charge. The introduction of electropositive boron into arenes causes an increase in energy of the occupied σ orbitals.[13] The expected strong donor ability of borabenzenes as ligands for transition metals was first observed experimentally by Schmid and co-workers with the preparation of Group 6 $M(CO)_3$ complexes of pyridine-borabenzene and pyridine-2-boranaphthalene, in which the CO stretching frequencies are markedly lower than in arene analogues.[15] The group of Fu (and later others) developed a general synthetic protocol for such borabenzene-base adducts,[14, 16-17] and showed that their coordination to $Cr(CO)_3$ dramatically increases the rate of nucleophilic aromatic substitution at boron.[18]

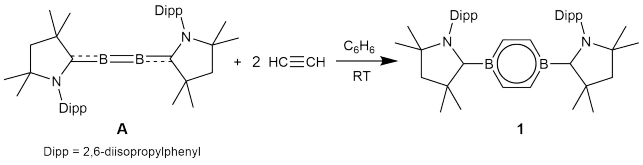

Scheme 1. Synthesis of diborabenzene **1**.

It follows that incorporation of further boron atoms into the arene ring (with associated Lewis base donors) should produce an even more strongly electron-donating ligand. Our reactivity studies on boron-boron multiply-bonded species recently provided a route to the first neutral, 6π-aromatic diborabenzene

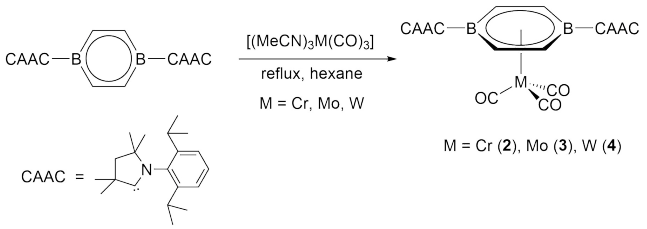

Scheme 2. Synthesis of compounds **2-4**.

compound, **1** (Scheme 1).[19] The species was accessed via reaction of diboracumulene **A** with excess acetylene. The apparent aromaticity of **1**, as well as the presence of benzene-like molecular orbitals according to DFT calculations, led us to explore its potential as an η^6 ligand for transition metals.

RESULTS AND DISCUSSION

Synthesis of 2-4. Reaction of the 1,4-bis(CAAC)-diborabenzene **1** with $[(MeCN)_3M(CO)_3]$ (M = Cr, Mo, W) in refluxing hexane afforded half-sandwich complexes $[(\eta^6$-**1**$)M(CO)_3]$ as black, crystalline solids in good yields (**2** (Cr): 55%; **3** (Mo): 62%; **4** (W): 66%) after recrystallisation from benzene (**Scheme 2**). Single-crystal X-ray diffraction confirmed the coordination of the heteroarene in each case. Compounds **2-4** are essentially isostructural in the solid state (**Figure 2**, Table 1). The diborabenzene ligand coordinates in an η^6 fashion to each of the metals, retaining its planarity. The flanking cyclic (alkyl)(amino)carbene (CAAC)[20] ligands display a *cis* conformation, as in the free ligand, and are somewhat twisted out of the diborabenzene plane. The bond distances in the ligand are identical within error over the three complexes, but significant differences are observed compared to the free diborabenzene. The B-C bonds to the CAAC substituent are extended by roughly 0.025 Å upon complexation, presumably reflecting a reduction in the π-donation from the aromatic ring to the CAAC moiety due to competition from the metal, while the ring C-C bonds are also slightly elongated. In each case, the metal sits slightly off-centre, with the bond distances to the ring carbon atoms adjacent to the bulky Dipp groups roughly 0.05 Å longer than those opposite. The distances from the ring centroid to the metal are essentially identical to those in the $[(\eta^6$-$C_6H_6)M(CO)_3]$ derivatives[21-23] and show the expected trend of Cr<W<Mo.

The ^{11}B NMR signals of the new compounds (6.0–7.0 ppm) are shifted significantly upfield from that of the free diborabenzene (**1**: 24.8 ppm). Analogously to the benzene derivatives,[24] the ring protons of the diborabenzene exhibit a significant shift in the ^{1}H NMR spectrum upon complexation, from 7.31 ppm to 4.74 (**2**), 4.97 (**3**) and 4.78 ppm (**4**). The ^{13}C NMR spectrum also reveals the expected large shifts from 150.5 ppm in **1** to 112.0 (**2**), 113.9 (**3**) and 109.3 ppm (**4**) for the ring carbon atoms, reflecting a reduction in aromaticity. The observation of a single resonance for the carbon and hydrogen atoms in the ring indicates free rotation about the B-C_{CAAC} bond in solution. The signals for the carbonyl groups appear at 243.8 (**2**), 232.6 (**3**) and 222.7 ppm (**4**), each shifted to significantly lower field than related $[(\eta^6$-arene$)M(CO)_3]$ complexes (between 227.0 and 238.5 ppm for Cr complexes) and indicative of exceptionally strong backbonding.[25-26]

Table 1. Selected crystallographically determined bond lengths (Å) and angles (°) in compounds **2-4**

	2	**3**	**4**
B1-C5	1.581(2)	1.582(4)	1.584(3)
B2-C9	1.587(2)	1.585(3)	1.581(3)
B1-C1	1.527(2)	1.530(3)	1.531(3)
C1-C2	1.397(2)	1.397(3)	1.403(3)
C2-B2	1.530(2)	1.528(3)	1.530(4)
B2-C3	1.526(2)	1.521(3)	1.528(4)
C3-C4	1.418(2)	1.424(3)	1.430(3)
C4-B1	1.524(2)	1.527(3)	1.517(3)
M-C13-15 (avg.)	1.827	1.947	1.952
M-ring centroid	1.725	1.904	1.891
Σ (C-**B1**-C)	359.9	360.0	359.7

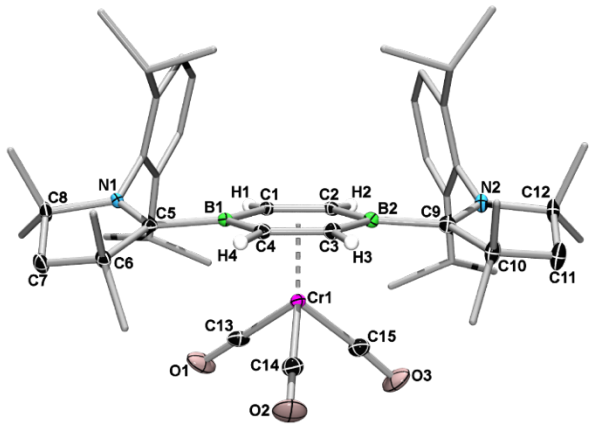

Figure 2. Crystal structure of compound **2** with atomic displacement ellipsoids shown at the 50% probability level. Hydrogen atoms, except H1-H4, have been removed for clarity.

Table 2. Carbonyl stretching frequencies of complexes **2-4** measured by infrared spectroscopy, alongside literature benchmarks, in cm^{-1}.

	2 (Cr)	**3** (Mo)	**4** (W)	$[(C_6H_6)Cr(CO)_3]$[7]	$[(py\text{-}C_5BH_5)Cr(CO)_3]$[15]
ν(CO)/ cm^{-1}	1880, 1788	1888, 1792	1884, 1792	1987, 1918	1925, 1850, 1805

IR and UV-vis Spectroscopy. In order to quantify the electron-donating properties of ligand **1**, we measured IR absorption spectra of compounds **2-4** to obtain the stretching frequen-

cies of the carbonyl ligands. The results are summarised in Table 2 alongside those of $[(C_6H_6)Cr(CO)_3]$[28] and Schmid's pyridine-borabenzene complex.[15] It is immediately clear that the diborabenzene complexes exhibit a large shift of the bands to lower energy. The A_1 and E carbonyl stretching frequencies of Cr complex **2** are 107 cm^{-1} and 130 cm^{-1} lower, respectively, than those of the parent benzene complex. To the best of our knowledge, these values represent the lowest CO frequencies yet observed for $[(\eta^6\text{-arene})M(CO)_3]$ complexes, implying remarkably strong backdonation from the (diborabenzene)M fragment into the π* orbitals of the CO ligands.

The UV-vis absorption spectra of **2**-**4** all display maxima around 400 nm (**2**: 424 nm, **3**: 412 nm, **4**: 400 nm), assigned to π-π* ligand transitions (see supporting information)). This represents a significant blue shift compared to **1** (633 nm). The bands shift to shorter wavelength as one moves down Group 6, consistent with stronger binding to the metal and increased stabilisation of the HOMO. Broad, lower intensity absorption bands are also observed at lower energy, presumably reflecting MLCT transitions.

Table 3. Interaction, Deformation and Binding Energies between the $M(CO)_3$ complexes and the diborabenzene ring calculated at the M06-L/def2-SVPD:PM6 level.

Term	**2**	**3**	**4**	$(C_6H_6)Cr(CO)_3$
Interaction Energy[a]	–92.2	–100.9	–103.6	–59.6
Deformation Energy	7.5	8.8	10.9	3.0
Binding Energy[b]	82.9	90.6	91.8	55.4

[a] BSSE correction included. [b] BSSE + ZPE corrections included.

Theoretical Calculations. In an attempt to gain more insight into the electronic properties of the new compounds, we performed density functional theory calculations to obtain the interaction and binding energies of the complexes. The interaction energies (complexation energies) were calculated as the energy difference between the total complex and the sum of fragments in its frozen geometry. Binding energies are the negative values of the dissociation energies (calculated as the total complex energy minus the energy of the fragments in its relaxed geometry). These results are shown in Table 3 alongside those of the parent compound, $[(\eta^6\text{-}C_6H_6)Cr(CO)_3]$ for comparison. The calculated binding energy of $[(\eta^6\text{-}C_6H_6)Cr(CO)_3]$ is 55.4 kcal·mol^{-1}, a value close to the experimental one of 53 kcal·mol^{-1}.[29] Thus, our computational results suggest that the interaction and binding energies between the diborabenzene and metal tricarbonyl fragments in these complexes (Cr: 82.9 kcal mol^{-1}, Mo: 90.6, W: 91.8) are considerably higher than in $[(\eta^6\text{-}C_6H_6)Cr(CO)_3]$. The interaction energies thus increase in the order Cr < Mo < W, as do the deformation energies, consistent with the expected trend of increasing bond strengths moving down the group.[29-30]

It is known that the complexation of $Cr(CO)_3$ to benzene decreases the aromaticity of the ring.[31] We therefore decided to calculate NICS(1) indices for the new complexes to follow the aromaticity trend. As expected, it decreases in the order [Cr]: –10.2, [Mo]: –9.5, [W]: –9.2, indicating lower aromaticity for the more strongly bound species.

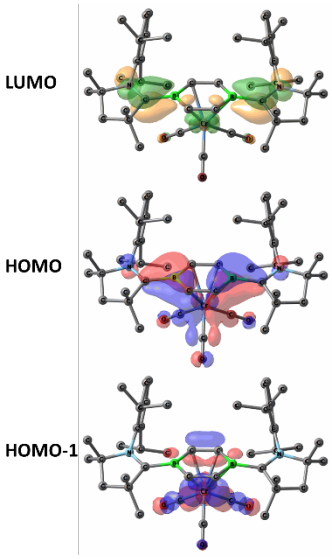

Figure 3. Frontier molecular orbital plots of compound **2** calculated at the meta-GGA M06-L level.

The HOMO describes mainly the interaction of the metal centre with the B-C bonds of the ligand, and the HOMO-1 is centered on the carbonyl bonding with the *d*-orbitals of the metal. This represents a marked difference to $[(\eta^6\text{-}C_6H_6)Cr(CO)_3]$, in which the HOMO is almost exclusively localized on the $Cr(CO)_3$ fragment.[32] The LUMO corresponds mainly to the π system of the B-C-N moiety of the CAAC ligands. These are destabilized with respect to the free ligand because the back-donation from boron is not effective, due to competition from the $M(CO)_3$ fragment. Moreover, we found that the CAAC ligands bend out of the diborabenzene plane toward the $M(CO)_3$ fragment. This angle follows the order [Cr]: 7.6°, [Mo]: 9.5°, [W]: 8.4°. This also corresponds to a small π-donation from the B-C_{CAAC} bonds to the metal centre (according to second-order perturbation theory analysis from NBO calculations, the stabilizing energies are [Cr]: 3.35 kcal mol^{-1}, [Mo]: 3.86, [W]: 1.62 for each B-C_{CAAC} bond). This also supports our observation of the strong electron-donating properties of the diborabenzene ring as a ligand.

Cyclic Voltammetry. The reactivity of arene chromium tricarbonyl complexes can be dramatically increased by oxidation or reduction of the substitutionally inert 18-electron species.[33] The compounds typically undergo an electrochemical one-electron oxidation to radical cations $[(\eta^6\text{-arene})Cr(CO)_3]^+$, whose stability depends strongly upon the nature of the electrolyte anion. The first crystal structure of such a complex, $[(\eta^6\text{-}C_6Me_6)Cr(CO)_3][B(C_6F_5)_4]$,[34] was reported in 2015 by utilizing an inert perfluoroaryl borate anion. Reduction results in a single two-electron process yielding dianions of the form $[(\eta^4\text{-arene})Cr(CO)_3]^{2-}$,[27, 35-36] in which a ring-slippage of the arene allows retention of the 18-electron configuration. We performed cyclic voltammetry experiments on complexes **2**-**4**, alongside $[(\eta^6\text{-}C_6H_6)Cr(CO)_3]$ for direct comparison. While

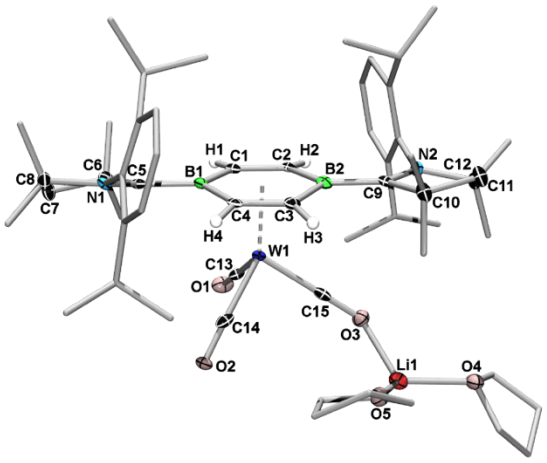

Figure 4 Crystal structure of compound **5** with atomic displacement ellipsoids shown at the 50% probability level. Hydrogen atoms, except H1-H4, have been removed for clarity.

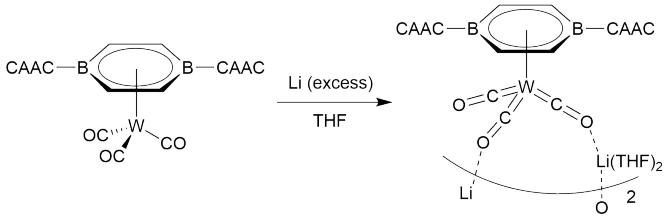

Scheme 3. Synthesis of compound **5**.

$[(\eta^6\text{-}C_6H_6)Cr(CO)_3]$ showed a single irreversible reduction at –3.07 V (vs. Fc/Fc^+), in broad agreement with literature reports,[27] each of the new diborabenzene complexes underwent a single oxidation and two independent reductions. All of the redox processes were found to be reversible under the CV conditions, with the exception of compound **4**, the cyclic voltammogram of which contained additional waves presumably linked to decomposition of the singly-reduced species. The values are displayed in Table 4, revealing similar behaviour for all three compounds, with a trend towards more positive potential as one moves down the group from Cr to W, i.e. that the chromium complex is the most easily oxidized but most difficult to reduce. The oxidation waves are shifted considerably from ca. 0.41 V for $[(\eta^6\text{-}C_6H_6)Cr(CO)_3]$ [37] to between –0.38 V (**4**) and –0.54 V (**2**). We attribute this discrepancy to the significant ligand contribution to the HOMO orbitals in **2**-**4**. The stepwise reduction is evidently favoured by the involvement of the B-CAAC moieties – CAACs are well known for their ability to stabilise radical species[38-39] – and population of the largely CAAC-based LUMO of **2**-**4** upon reduction would avoid the formation of an unstable $19e^-$ metal centre.

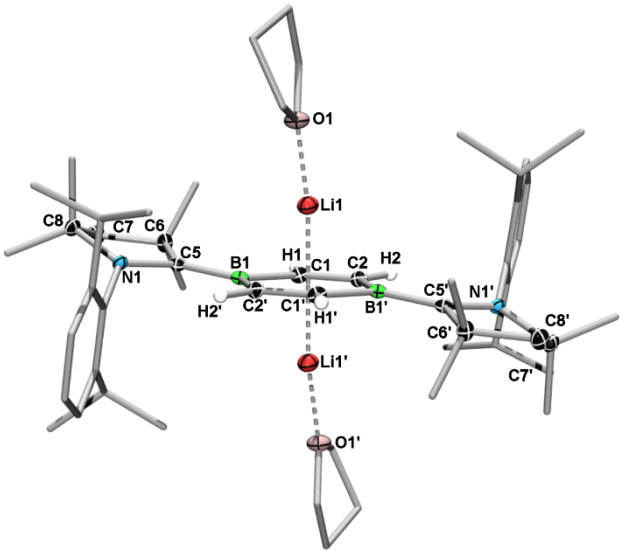

Figure 5 Crystal structure of compound **6a** with selected atomic displacement ellipsoids at the 50% probability level. Hydrogen atoms except for H1 and H2 are omitted for clarity.

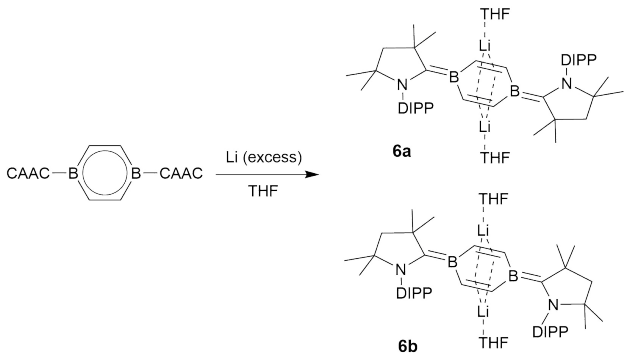

Scheme 4. Synthesis of compounds **6a**/**6b**.

Table 4. Oxidation potentials of compounds **2**-**4** in V vs. Fc/Fc^+.

	2	**3**	**4**	**$(C_6H_6)Cr(CO)_3$**
Oxidation	**–0.54**	**–0.41**	**–0.38**	**0.41**[a]
1st reduction	**–2.33**	**–2.26**	**–2.25**	**–3.07**[b]
2nd reduction	**–2.96**	**–2.93**	**–2.89**	**–3.07**[b]

[a] Taken from reference [40]. [b] Single reduction wave observed.

Chemical Reduction. With the knowledge that **2**-**4** can be reduced to stable compounds, we were keen to isolate a reduced species. Reaction of tungsten complex **4** with excess Li metal in THF led to a black, paramagnetic solution (**Scheme 3**). The EPR spectrum of the solution showed a poorly resolved signal at $g_{iso} = 1.996$, consistent with a largely ligand-centred spin distribution (see ESI). Due to the large spin-orbit coupling constant of tungsten, a higher metal contribution would be reflected in g_{iso} values that are significantly lower than that of the free electron.[41] The simulated hyperfine coupling constants of 8.3 (^{14}N), 8.5 (^{1}H), and 5.1 MHz (^{11}B) for the diborabenzene ligand as

well as the small tungsten coupling of $a(^{183}W) \approx 10$ MHz, obscured by the linewidth, confirm the picture of a mainly ligand-based radical.

X-ray diffraction on single crystals obtained from a benzene solution confirmed the formation of the radical anion [(**1**)W(CO)$_3$]Li·2THF (**5**, **Figure 4**). The compound is dimeric in the solid state, with CO···Li$^+$···OC interactions connecting the two fragments. Unfortunately, the data obtained are inadequate for a discussion of further structural parameters. Although the EPR signal of **5** was reproducible, attempts to isolate the compound in bulk were unsuccessful owing to its instability. After several hours, ^{11}B NMR signals reappeared for **4** and what was later identified as **6** (see below), among other unidentified species, suggesting the action of a disproportionation pathway. Nonetheless, compound **5** represents to the best of our knowledge the first example of a monoanionic arene tricarbonyl complex of a Group 6 metal.

Remarkably, we discovered that the reduction of **1** does not require coordination to a transition metal fragment. Reaction of **1** with lithium metal for 5 d provides the dianion as its dilithium compound, Li$_2$(THF)$_2$[**1**] (**6**) in 68% yield (**Scheme 4**). The compound has a deep purple colour in solution, appearing black in the solid state. Single-crystal X-ray diffraction confirmed the composition of **6** (**Figure 5**). The B-CAAC bonds (1.498(3) Å) are markedly shortened with respect to **1**, while the ring B-C bonds (1.561(3), 1.569(3) Å) are lengthened, indicating a quinoid-type structure. The lithium atoms sit centrally upon the ring, each coordinated by one THF ligand. While a single peak is observed for **6** in the ^{11}B NMR spectrum at 13.6 ppm, the ^{1}H and ^{13}C NMR spectra revealed the presence of two compounds in a 2:1 ratio. We postulated the formation of two isomers, **6a** and **6b**, with opposing double bond geometry. This assumption was supported by ^{1}H NOESY NMR spectroscopy, which revealed through-space coupling between the methyl and *iso*-propyl substituents of the CAAC moiety with the appropriate hydrogen atoms on the central ring. Optimisation of the two structures by DFT (B3LYP/6-311G(d)) revealed them to be of very similar energy, with **6a** favoured by 1.35 kcal·mol^{-1}. Variable temperature NMR studies showed broadening of the **6a**/**6b** signals at 90 °C, but a coalescence temperature could not be determined. This observation is consistent with a high barrier to interconversion, and therefore significant B-CAAC π-bonding, providing further support for a quinoidal structure. Reaction of **6a**/**6b** with $ZrCl_4$ resulted in quantitative regeneration of **1** alongside elemental Zr, supporting the formulation as stereoisomers and illustrating the high reduction potential of **6**.

Interestingly, compound **6** is also obtained from the lithium reduction of chromium complex **2**, indicating an increased lability of the ligand in its reduced form and providing experimental support for the calculated trend in ligand binding energies. The only stable benzene-derived dianions known are highly conjugated[42-43] or sterically and electronically stabilized by multiple bulky silyl groups;[44-46] in the case of **1**, the ability of the CAAC moieties to accept π-electron density from the ring leads to the stability of the highly reduced species **6**.

Conclusions We have prepared half-sandwich complexes of the group VI metals with a diborabenzene ligand (**2**-**4**). The carbene-stabilised diborabenzene ligand is shown to be a considerably stronger electron donor than its all-carbon analogues, with carbonyl stretching frequencies unprecedentedly low for neutral piano stool complexes. The redox chemistry of the new complexes is divergent from that of arene complexes, with cyclic voltammetry and DFT calculations revealing reversible and largely ligand-centred oxidation and reduction processes. Reduction of neutral complex **4** with lithium provided evidence of a monoanionic diborabenzene tungsten tricarbonyl complex, **5**. Furthermore, it was possible to reduce the free diborabenzene to its dianion, **1**$^{2-}$. The stability of **1** in multiple oxidation states promises a rich coordination chemistry, and considering the burgeoning research field of redox-active ligands,[47-48] we are confident that ligand **1** may find applications in homogeneous catalysis.

ASSOCIATED CONTENT

Supporting Information including full experimental details, spectra, crystallographic files (CIF) and computational details. This material is available free of charge via the Internet at http://pubs.acs.org.

AUTHOR INFORMATION

Corresponding Author

*h.braunschweig@uni-wuerzburg.de

ACKNOWLEDGMENTS

This project has received funding from the European Research Council (ERC) under the European Union Horizon 2020 Research and Innovation Program (grant agreement no. 669054). J.O.C.J.-H. thanks CONACyT through project CB2014-241803 for his research stay at the Julius-Maximilians-Universität Würzburg.

REFERENCES

1. Semmelhack, M. F., In *Comprehensive Organometallic Chemistry II*, Abel, E. W.; Stone, F. G. A.; Wilkinson, G., Eds. Pergamon: New York, 1995; Vol. 12.
2. Rosillo, M.; Dominguez, G.; Perez-Castells, J., *Chem. Soc. Rev.* **2007,** *36*, 1589-1604.
3. Dimroth, K.; Thamm, R.; Kaletsch, H., *Z. Naturforsch. B.* **1984,** *39*, 207-212.
4. Schmidt, R.; Massa, W., *Z. Naturforsch. B.* **1984,** *39*, 213-216.
5. Deberitz, J.; Nöth, H., *Chem. Ber.* **1970,** *103*, 2541-2547.
6. Vahrenkamp, H.; Nöth, H., *Chem. Ber.-Recueil* **1972,** *105*, 1148-1157.
7. Dimroth, K.; Luckoff, M.; Kaletsch, H., *Phosphorus Sulfur Silicon Rel. Elem.* **1981,** *10*, 285-294.
8. Märkl, G.; Baier, H.; Liebl, R.; Mayer, K., *J. Organomet. Chem.* **1981,** *217*, 333-356.
9. Ashe, A.; Colburn, J., *J. Am. Chem. Soc.* **1977,** *99*, 8099-8100.
10. Shinohara, A.; Takeda, N.; Sasamori, T.; Matsumoto, T.; Tokitoh, N., *Organometallics* **2005,** *24*, 6141-6146.
11. Nakata, N.; Takeda, N.; Tokitoh, N., *Angew. Chem. Int. Ed.* **2003,** *42*, 115-117.
12. Su, B.; Kinjo, R., *Synthesis* **2017,** *49*, 2985-3034.
13. Herberich, G.; Ohst, H., *Adv. Organomet. Chem.* **1986,** *25*, 199-236.
14. Fu, G., *Adv. Organomet. Chem.* **2001,** *47*, 101-119.
15. Boese, R.; Finke, N.; Keil, T.; Paetzold, P.; Schmid, G., *Z. Naturforsch. B.* **1985,** *40*, 1327-1332.
16. Hoic, D.; Wolf, J.; Davis, W.; Fu, G., *Organometallics* **1996,** *15*, 1315-1318.
17. Légaré, M.; Bélanger-Chabot, G.; De Robillard, G.; Languérand, A.; Maron, L.; Fontaine, F., *Organometallics* **2014,** *33*, 3596-3606.

18. Qiao, S.; Hoic, D.; Fu, G., *J. Am. Chem. Soc.* **1996,** *118*, 6329-6330.
19. Arrowsmith, M.; Böhnke, J.; Braunschweig, H.; Celik, M.; Claes, C.; Ewing, W.; Krummenacher, I.; Lubitz, K.; Schneider, C., *Angew. Chem. Int. Ed.* **2016,** *55*, 11271-11275.
20. Soleilhavoup, M.; Bertrand, G., *Acc. Chem. Res.* **2015,** *48*, 256-266.
21. Farrugia, L.; Evans, C.; Lentz, D.; Roemert, M., *J. Am. Chem. Soc.* **2009,** *131*, 1251-1268.
22. Bürgi, H.; Raselli, A.; Braga, D.; Grepioni, F., *Acta Crystallogr. B* **1992,** *48*, 428-437.
23. Oh, J.; Geib, S.; Cooper, N., *Acta Crystallogr. C* **1998,** *54*, 581-583.
24. Solladie-Cavallo, A., *Polyhedron* **1985,** *4*, 901-927.
25. Mann, B., *J. Chem. Soc. Dalton Trans.* **1973**, 2012-2015.
26. Hunter, A.; Mozol, V.; Tsai, S., *Organometallics* **1992,** *11*, 2251-2262.
27. Dessy, R.; Stary, F.; King, R.; Waldrop, M., *J. Am. Chem. Soc.* **1966,** *88*, 471-476.
28. Brown, D.; Raju, J., *J. Chem. Soc. A.- Inorg. Phys. Theor.* **1966**, 1617-1620.
29. Mukerjee, S.; Lang, R.; Ju, T.; Kiss, G.; Hoff, C.; Nolan, S., *Inorg. Chem.* **1992,** *31*, 4885-4889.
30. Smith, G., *Polyhedron* **1988,** *7*, 1605-1608.
31. Feixas, F.; Jiménez-Halla, J.; Matito, E.; Poater, J.; Sola, M., *Pol. J. Chem.* **2007,** *81*, 783-797.
32. Cheng, H.; Chang, J.; Shih, C., *J. Phys. Chem. A.* **2010,** *114*, 2920-2929.
33. Geiger, W., *Coord. Chem. Rev.* **2013,** *257*, 1459-1471.
34. Wang, W.; Wang, X.; Zhang, Z.; Yuan, N.; Wang, X., *Chem. Commun.* **2015,** *51*, 8410-8413.
35. Rieke, R.; Arney, J.; Rich, W.; Willeford, B.; Poliner, B., *J. Am. Chem. Soc.* **1975,** *97*, 5951-5953.
36. Wey, H.; Butenschön, H., *Angew. Chem. Int. Ed.* **1990,** *29*, 1444-1445.
37. Stone, N.; Sweigart, D.; Bond, A., *Organometallics* **1986,** *5*, 2553-2555.
38. Martin, C.; Soleilhavoup, M.; Bertrand, G., *Chem. Sci.* **2013,** *4*, 3020-3030.
39. Bissinger, P.; Braunschweig, H.; Damme, A.; Krummenacher, I.; Phukan, A.; Radacki, K.; Sugawara, S., *Angew. Chem. Int. Ed.* **2014,** *53*, 7360-7363.
40. Yeung, L. K.; Kim, J. E.; Chung, Y. K.; Rieger, P. H.; Sweigart, D. A., *Organometallics* **1996,** *15*, 3891-3897.
41. Goodman, B. A.; Raynor, J. B., *Adv. Inorg. Chem. Radiochem.* **1970,** *13*, 135-362.
42. Jesse, R.; Biloen, P.; Prins, R.; Vanvoorst, J.; Hoijtink, G., *Mol. Phys.* **1963,** *6*, 633-635.
43. Gherghel, L.; Brand, J.; Baumgarten, M.; Mullen, K., *J. Am. Chem. Soc.* **1999,** *121*, 8104-8105.
44. Sekiguchi, A.; Ebata, K.; Kabuto, C.; Sakurai, H., *J. Am. Chem. Soc.* **1991,** *113*, 1464-1465.
45. Ebata, K.; Setaka, W.; Inoue, T.; Kabuto, C.; Kira, M.; Sakurai, H., *J. Am. Chem. Soc.* **1998,** *120*, 1335-1336.
46. Setaka, W.; Ebata, K.; Sakurai, H.; Kira, M., *J. Am. Chem. Soc.* **2000,** *122*, 7781-7786.
47. Luca, O.; Crabtree, R., *Chem. Soc. Rev.* **2013,** *42*, 1440-1459.
48. Praneeth, V.; Ringenberg, M.; Ward, T., *Angew. Chem. Int. Ed.* **2012,** *51*, 10228-10234.